Harmonic Synchrophasors Measurement Algorithms with Embedded Compensation of Voltage Transformer Frequency Response

Paolo Castello, *Member*, *IEEE*, Christian Laurano, *Member*, *IEEE*, Carlo Muscas, *Senior Member*, *IEEE,* Paolo Attilio Pegoraro, *Senior Member*, *IEEE*, Sergio Toscani, *Senior Member*, *IEEE*, Michele Zanoni, *Member*, *IEEE.*

***Abstract*— The widespread diffusion of nonlinear power electronics-based devices in distribution grids has raised the interests towards power quality monitoring. In this respect, the estimation of synchronized harmonic phasors would enable the employment of algorithms that allow identifying the sources of harmonic disturbances, which, until now, have been only tested through numerical simulations or implemented in small-scale. However, the impact of the uncertainty due to the employed voltage transformers and to the other devices that compose the measurement chain has to be analyzed. In this framework, the present paper proposes a class of harmonic synchrophasor estimation algorithms that allows compensating the frequency response function of the instrument transformer. The technique has been tested and validated under realistic conditions considering an inductive voltage transformer. Experimental results highlight its effectiveness, especially when taking into account its ease of implementation. The black-box approach allows abstracting from the operating principle of the voltage transducer.**

Keywords—Instrument transformers; Synchronized measurements; Voltage transformers; Harmonics; Measurement uncertaninty

I. INTRODUCTION

Nowadays we are experiencing a drastic increase of power electronics components in ac distribution grids. Technological advancement has dramatically improved the performance of semiconductor devices; as a result, the number of loads connected to the grid through power electronics converters is continuously rising. On the other hand, most of the generators from renewable sources, such as wind turbines and photovoltaic plants, must be connected by means of proper interface converters. Their nonlinear behaviour introduces harmonic disturbances in voltage and current waveforms.

Harmonic pollution represents one of the most severe power quality (PQ) issues [1], since it produces additional losses (thus resulting in increased heating and lower efficiency), accelerates aging of materials and may trigger resonances with potentially harmful consequences. For this reason, the interest towards harmonic monitoring and harmonic state estimation [2]-[4] has recently increased. Reconstructing the harmonic state of the grid would permit identifying disturbing devices [5]-[7] as well as studying possible remedies. However, reliable and time-tagged harmonic measurements are required for the purpose. In this context, recent papers have extended the concept of synchrophasor [8] (initially intended for the fundamental term) to the harmonic components, thus leading to the concept of harmonic synchrophasor [9].

The outcome of the harmonic state estimation strongly depends on the quality of the input data, thus on the accuracy of the measured harmonic synchrophasors. A significant uncertainty contribution may come from the algorithm employed to extract the phasors; for example, it may suffer from spectral leakage under off-nominal frequency conditions or accuracy may be degraded by measurement noise. Furthermore, it should be noticed that voltage and current signals are measured by means of instrument transformers (ITs), which convert the electric quantities into voltage signals that have to be properly acquired and processed; these ITs add significant uncertainty to the overall measurement result [10]. For example, let us consider harmonic voltage measurements in medium voltage distribution grids: conventional inductive voltage transformers (VTs) are widely employed to this purpose, although their metrological performance is guaranteed only at the fundamental component [11]. As a consequence, in general the accuracy of harmonic measurements does not comply with the rated ratio and phase errors of the VT, either because of bandwidth limitations [12]-[14] and nonlinearities produced by core magnetization [15]-[17].

Several techniques aimed at extending the measurement bandwidth of VTs thanks to proper winding design [18] or through post-compensation filters [19], [20] have been proposed. Methods able to mitigate also nonlinear effects are recently emerging [21], [22]; of course, their implementation is considerably more complex.

When considering harmonic synchrophasor measurements, it would be extremely interesting to directly integrate these techniques at instrument design stage, allowing one to partially compensate the error contributions due to the VT into the estimation algorithm. In this respect, [23] provided a first scouting of the idea, focused on the analysis of the impact of the two main error sources. In this paper, the main contribution is the proposal of an improved frequency-domain linear compensation method, which is highly integrated with the harmonic synchrophasor measurement algorithm and based on synchronized frequency measurements. The performance achieved by the proposed solution has been evaluated through an extensive experimental activity that proves the advantages of the new concept.

The paper is organized as follows: Section II introduces the harmonic synchrophasor measurement considering the VT, presents the proposed frequency domain compensation

P. Castello, C. Muscas and P. A. Pegoraro are with the Department of Electrical and Electronic Engineering, University of Cagliari, 09123 Cagliari, Italy (e-mail: paolo.pegoraro@unica.it).

C. Laurano, S. Toscani and M. Zanoni are with the Dipartimento di Elettronica, Informazione e Bioingegneria, Politecnico di Milano, 20133 Milan, Italy (e-mail: sergio.toscani@polimi.it).

and its integration with the synchrophasor estimation algorithm; Section III and Section IV describe the experimental setup and the VT frequency response identification process, respectively; Section V reports and analyses the experimental results while Section VI concludes the paper with some final considerations.

II. Synchronized Harmonic Phasor Measurements

Synchronized phasor measurements have become a reality in transmission system monitoring with the design and installation of Phasor Measurement Units (PMUs) [24], which provide frequent and time-synchronized (with respect to coordinated universal time, UTC) fundamental phasor measurements from voltage and current signals, along with frequency and Rate of Change of Frequency (ROCOF) [8]. The synchronization is typically obtained thanks to Global Positioning System receivers integrated into the measurement device or from a master source via Precision Time Protocol, through an Ethernet network.

Nowadays, the interest toward PMU technology is moving also to the distribution level. Considering distribution grids, synchronized phasor measurements can be also exploited for diffuse PQ analysis, in which the data acquired from different positions have to be compared. In this scenario, the use of synchronized harmonic phasors to identify the sources of the harmonic disturbances has been proposed [7], [25]. The measurement of harmonic synchrophasors is rather challenging, and it cannot be obtained by simply exploiting the procedures that are used in the conventional PQ instruments or PMUs.

In fact, on the one hand instruments compliant with the most recent standard for PQ measurement methods [26] are not meant to provide any kind of information about the absolute phases of the harmonic components. A reference to UTC is requested by [26], but it is aimed at time-tagging the measurements, in order to allow proper comparison of PQ parameters measured in different nodes of the grid. For this reason, the required time-clock accuracy is 20 ms (for class A instruments and 50-Hz systems), which is definitely useless for synchrophasor measurements. On the other hand, the current standard on synchrophasors [27] only focuses on the fundamental component, while harmonics are merely considered as disturbances to be filtered out.

Thus, in order to extend the functionality of the PMU to estimate also synchronized harmonic phasors (harmonic PMU, h-PMU), suitable specific approaches are mandatory. In this context, different algorithms have been proposed (see for instance [25], [28] and [29]). The most common methods are based on DFT, but other estimation techniques can be found in the literature, e.g. based on Taylor-Fourier transform [30], invariance technique [31] and Kalman filtering [28], [32]. These methods focus on the harmonic extraction from the electric signal, but, in this paper, the interest is on the overall performance achievable with the measurement chain composed of IT and h-PMU and on the design of a h-PMU that is "IT aware".

A. Impact of the instrument transformer

Let us suppose that the target is evaluating voltage harmonic synchrophasors in a node of a distribution grid. In general, the PMU is connected to the grid through proper ITs, each one characterized by a relationship between primary and secondary harmonics ($V_1(h)$ and $V_2(h)$ respectively, h denotes the harmonic order). Therefore, primary voltage harmonic synchrophasors $V_{1,E}(h)$ have to be reconstructed by means of a proper mapping function from the output of the estimation algorithm, $V_{2,E}(h)$, as shown in Fig. 1.

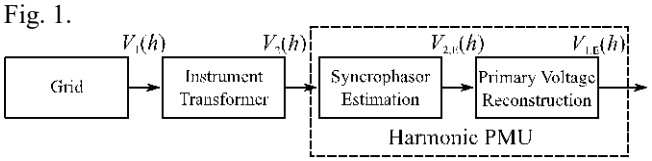

Fig. 1. Measurement of harmonic synchrophasors: block diagram.

It has to be stressed that the mismatch between the actual behavior of the IT and the mapping function used to perform measurements introduces an additional uncertainty contribution that has to be properly taken into account. For example, let us suppose that a conventional inductive VT is employed. Considering a frequency range up to few kilohertz, while assuming that the secondary burden is close to its rated value, capacitive effects can be neglected. Therefore, its behavior can be accurately represented with the usual Steinmetz equivalent circuit shown in Fig. 2:

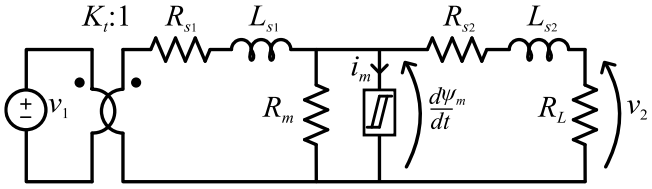

Fig. 2. Equivalent circuit of the VT.

All the parameters have been reported to the secondary side; v_1 and v_2 are the primary and secondary voltages, K_t the turn ratio, R_{s1} and R_{s2} represent the primary and secondary winding resistances, L_{s1} and L_{s2} the primary and secondary winding leakage inductances. Core magnetization can be modeled with a quasi-steady-state hysteretic relationship $i_m(\psi_m)$, where i_m is the magnetizing current and ψ_m the mutual flux linkage; eddy current loss is considered with the parallel resistor R_m. Resistive burden is assumed, thus modeled with resistor R_L.

Considering the previous circuit model, the secondary voltage waveform v_2 is not just a scaled replica of the primary voltage v_1 according to the nominal ratio K_n provided by the manufacturer. First of all, it is affected by the dynamic behavior of the transformer. However, v_2 also suffers from nonlinear effects: because of the iron core, the relationship between primary voltage and magnetizing current is nonlinear; in turn, this results in a small distorted voltage drop across the primary winding series parameters, thus introducing a weak nonlinearity in the relationship between v_1 and v_2. This nonlinear effect is typically negligible at the fundamental component.

As far as harmonic synchrophasor measurements are concerned, the non-ideal behavior of the IT has to be taken into account when the mapping function is selected. Techniques that allow partially compensating for the nonlinearities introduced by VTs have been proposed in the literature, but the focus of this paper is on a linear reconstruction of the primary voltage from the secondary side, which is effective, as shown in the following, and computationally light. As aforementioned, a VT is nonlinear, but each nonlinear system can be decomposed into an underlying linear system and a nonlinear part. This underlying linear system sets a relationship between primary and secondary voltage, which can be expressed in terms of a transfer function $F(s)$:

$$F(s)=\frac{V_2(s)}{V_1(s)} \quad (1)$$

where $V_1(s)$ and $V_2(s)$ are the Laplace transforms of the primary and secondary voltage, respectively. When substituting $s=j\omega$ in (1), the relationship between primary and secondary voltage spectral components due to the underlying linear system is obtained; $F(j\omega)$ represents its frequency response function (FRF), which can be considered as an approximated model of the employed VT. Assuming that we have an estimate of $F(j\omega)$, the primary voltage harmonic synchrophasors can be reconstructed from the secondary side by using its inverse $G(j\omega)$, thus compensating the artifacts introduced by the underlying linear system.

Now, let us consider again the circuit model of the inductive VT reported in Fig. 2. Assuming linearity, the mutual flux linkage ψ_m is proportional to the magnetizing current i_m according to the magnetizing inductance L_m. By performing calculation, the relationship between primary and secondary voltage is represented by a minimum phase, 3rd order transfer function $F(s)$ having one zero in the origin due to core magnetization.

B. Harmonic synchrophasor estimation algorithm

In this paper, a new proposal for an integrated synchronized harmonic estimation and VT compensation is presented. In the following, the main idea of the measurement procedure is explained, and the measurement algorithm adopted in the next Section V is briefly described.

The concept at the basis of the proposal is schematically illustrated in Fig. 3. The acquired secondary voltage samples are elaborated to obtain an estimate $V_{2,E}(h)$ of the secondary voltage harmonic synchrophasors and of the fundamental frequency $f_{0,E}$. In turn, $f_{0,E}$ is used to compute the frequency response compensation of the VT in the estimated harmonic grid at runtime and, finally, the compensation is applied to $V_{2,E}(h)$ in order to reconstruct the primary voltage harmonics.

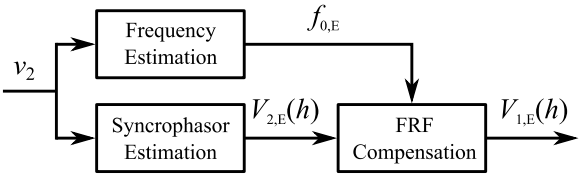

Fig. 3. Harmonic synchrophasor estimation scheme.

For the analysis performed in this paper, which is focused on steady-state signals, the harmonic synchrophasor estimation algorithm is a two-step procedure:

1. A discrete Fourier transform (DFT) is applied to a window of N_{c1} nominal-frequency cycles weighted through a Low Sidelobe window (LSW), which belongs to the generalized-cosine family, defined by the following coefficients:

$$w[n]=\sum_{k=0}^{4}(-1)^k a_k \cos\frac{2\pi kn}{L} \quad (2)$$

Where L is the window length while a_k, for k=0,2,3,4 are, respectively, 0.471492057, 0.17553428, 0.028497078, 0.001261367. The DFT is used to compute only the bin corresponding to the rated fundamental frequency. Its phase-angle is then used to compute a centered discrete-time derivative (as in [24]) thus obtaining an estimation of the frequency.

2. The discrete time Fourier transform (DTFT) is evaluated for each harmonic frequency of interest, belonging to a frequency grid that is tuned using the frequency estimated in the first step in order to reduce leakage-related artifacts. The DTFT is applied to a N_{c2} cycle window. A different weighting window with respect to the first step can be generally applied, but, in Section V, the same samples already weighted by the LSW are used.

The compensation process relies on the evaluation of the compensation FRF $G(j\omega)$ on a proper harmonic grid, according to the estimated fundamental frequency. These values are used to multiply the estimated secondary side harmonic synchrophasors $V_{2,E}(h)$, thus obtaining the primary values $V_{1,E}(h)$. The whole estimation process is performed on sample-by-sample basis by shifting the analysis window.

III. Experimental Setup

The target of the present paper is evaluating the accuracy improvement which can be achieved in harmonic synchrophasor measurements as long as a linear compensation of the instrument transformer is introduced. As a case study, a low voltage VT is considered; its rated specifications are reported in Table I. The secondary winding has been connected to the rated resistive burden.

TABLE I. Voltage transformer specifications

V_{1n} [V]	V_{2n} [V]	f_n [Hz]	Class	Burden [VA]
200	100	50	0.5	20

The activity requires a proper experimental setup that allows identifying the FRF of the VT, while applying periodic multitone primary waveforms in order to assess the performance under realistic conditions. Primary and secondary waveforms have to be measured with adequate accuracy. The adopted architecture resembles that presented in [33] and is reported in Fig. 4.

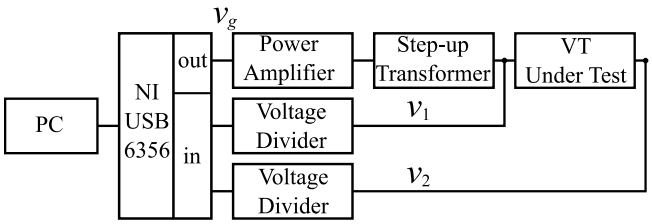

Fig. 4. Diagram of the experimental setup.

The primary voltage of the VT under test has been provided by an AE Techron 7548 industrial power amplifier (specifications are reported in Table II) connected to a 100V/400V transformer in order to increase its maximum output voltage capability. Primary and secondary voltage waveforms have been measured by using properly calibrated resistive voltage dividers; they have been connected as close as possible to the terminals of the VT under test by means of twisted cables. Analog Devices AD215BY isolation amplifiers configured as voltage followers provide galvanic insulation. The frequency responses of the two measurement channels have been measured and compensated, so that the relative gain mismatch is below 10^{-4} while the phase mismatch is lower than 0.1 mrad between 50 Hz and 1250 Hz.

TABLE II. POWER AMPLIFIER SPECIFICATIONS

V_{max} [V]	I_{max} [A]	Bandwidth	THD	SNR [dB]
200	43	DC-30 kHz (+0.1, -0.5 dB)	<0.1%	>120

The input signal for the power amplifier and the data acquisition of the primary and secondary voltage signals has been provided by a National Instruments NI USB-6356 board featuring 16-bit resolution, simultaneous sampling and generation capability, and adjustable full-scale range. A sampling rate f_s=100 kHz has been employed during the tests. Generation and data acquisition processes have been managed by a PC running proper Matlab scripts.

As mentioned above, the previously described experimental setup has been adopted to apply periodic multisine primary voltages to the VT under test, namely characterized by a fundamental frequency f_0 and harmonics up to the Nth order. For avoiding aliasing artifacts, f_0 (e.g. 50 Hz) must be a divider of the sampling rate, thus resulting in an integer number of samples per fundamental period. It is worth noting that mainly because of the step-up transformer, the primary voltage waveform $v_1(t)$ is not just a scaled up replica of the signal $v_g(t)$ at the input of the power amplifier. In order to mitigate this problem, before applying the test waveforms, a small amplitude random phase multisine signal having fundamental frequency f_0 and all the harmonics up to the Nth order has been applied. This allows evaluating the frequency response function between $v_g(t)$ and $v_1(t)$ on the harmonic grid, which can be inverted to pre-distort in the frequency domain the multisine test signal to be applied, thus compensating the filtering behavior of the generation system. Further details about the generator are reported in [33]; it can be employed to generate generic periodic multisine signals, as used here both to measure the FRF of the VT (Section IV) and to test the proposed method (Section V). Of course, nonlinear effects cannot be mitigated, but they are hopefully rather small. On the other hand, a slight deviation of the actual primary voltage waveform with respect to its reference value has a negligible impact on the achieved results, since this voltage has been measured with a reference transducer.

IV. IDENTIFYING THE VT FRF

In order to implement the proposed compensation technique, the FRF of the considered VT has to be evaluated. First of all, the response at the rated frequency has been measured through a conventional calibration. It is well known that, for best results, the amplitude of the fundamental primary voltage should be close to that occurring during normal operation. In this way, the FRF coefficient is able to partly embed some of the so-called systematic nonlinear effects. Therefore, the voltage generator has been used to apply a sinusoidal primary voltage having rated amplitude and frequency f_n=50 Hz, corresponding to the angular frequency $\omega_n=2\pi f_n$. P=500 periods of the primary and secondary voltage waveforms have been acquired under steady-state conditions; for the generic pth period (p =1…P), the fundamental components $V_{1,cal}^{[p]}(j\omega_n)$ and $V_{2,cal}^{[p]}(j\omega_n)$ have been extracted through DFT. Let us assume that the impact of measurement error on the evaluated primary and secondary voltage spectral components can be modeled as additive zero-mean, complex-valued random variables $\Delta V_{1,cal}(j\omega_n)$ and $\Delta V_{2,cal}(j\omega_n)$. Each spectral component obtained starting from the pth period is assumed to be affected by an independent realization of the aforementioned random contribution. Under this hypothesis, its impact can be significantly reduced by averaging over the P periods, thus obtaining $V_{1,cal}(j\omega_n)$ and $V_{2,cal}(j\omega_n)$.

A reasonable assumption is that $\Delta V_{1,cal}(j\omega_n)$ and $\Delta V_{2,cal}(j\omega_n)$ have jointly circularly symmetric complex normal distribution. In this respect, their statistical behavior is expressed by three parameters: their variances $\sigma_{1,cal}^2(j\omega_n)$, $\sigma_{2,cal}^2(j\omega_n)$ and the covariance $\sigma_{12,cal}^2(j\omega_n)$ which can be estimated from the experimental data by considering each period as an independent random realization. The maximum likelihood (ML) estimate of the FRF [34] at the rated fundamental frequency, namely $F_{np}(j\omega_n)$, is computed as:

$$F_{np}\left(j\omega_n\right)=\frac{V_{2,cal}\left(j\omega_n\right)}{V_{1,cal}\left(j\omega_n\right)} \tag{3}$$

Assuming high signal to noise ratio (SNR), also $F_{np}(j\omega_n)$ is affected by a random additive contribution having circular symmetric complex normal distribution. Its parameter $\sigma_F(j\omega_n)$ (thus corresponding to the standard deviation of the real and imaginary part) results [34]:

$$\sigma_F\left(j\omega_n\right)=\frac{\left|F_{np}\left(j\omega_n\right)\right|}{\sqrt{P}}\sqrt{\frac{\sigma_{1,cal}^2\left(j\omega_n\right)}{\left|V_{1,cal}\left(j\omega_n\right)\right|^2}+\frac{\sigma_{2,cal}^2\left(j\omega_n\right)}{\left|V_{2,cal}\left(j\omega_n\right)\right|^2}+-2\Re\left[\frac{\sigma_{12,cal}^2\left(j\omega_n\right)}{V_{1,cal}\left(j\omega_n\right)V_{2,cal}^{*}\left(j\omega_n\right)}\right]} \tag{4}$$

Thanks to the experimental setup and to frequency domain averaging, $\sigma_F(j\omega_n)$ is extremely small, below -110dB in relative value.

After that, the FRF of the VT has been evaluated at the multiples of the rated fundamental frequency. In this case, it is mandatory to avoid nonlinear effects that may bias the estimates. The voltage generator has been employed to apply a random phase multisine signal having rated fundamental frequency and containing harmonics whose order h ranges from 2 to 26; all the spectral components share the same amplitude. The overall root mean square (rms) value of the excitation signal is below 10% of the rated primary voltage: core flux is much lower than its rated value and thus nonlinear effects are supposed to be very small. P=500 periods of the primary and secondary voltage waveforms have been acquired under steady-state conditions. The DFT has been computed for each period p of the two signals, thus obtaining $V_{1,cal}^{[p]}(jh\omega_n)$ and $V_{2,cal}^{[p]}(jh\omega_n)$. Under the same assumptions that have been introduced when discussing the calibration at rated frequency, averaging over the periods can be employed for each hth harmonic to reduce the effect of noise; variances $\sigma_{1,cal}^2(jh\omega_n)$, $\sigma_{2,cal}^2(jh\omega_n)$ and covariance $\sigma_{12,cal}^2(jh\omega_n)$ can also be computed. Equation (3) can be used to obtain the ML estimate of the FRF at angular frequencies $h\omega_n$, while (4) allows evaluating $\sigma_F(jh\omega_n)$ which quantifies the impact of measurement noise; its relative value is below -100 dB.

The previously described procedure allows obtaining $F_{np}(jh\omega_n)$, namely a nonparametric estimate of the FRF evaluated on a harmonic grid. Its inverse $G_{np}(jh\omega_n)$ permits reconstructing the primary voltage harmonics from the secondary side; however, it cannot be evaluated outside of the harmonic grid. In order to overcome this issue, a parametric model $G_p(s,\Pi)$ of the inverse transfer function can be introduced. The set Π of the transfer function parameters

(e.g. the gain and the location of its poles and zeros in the complex plane), can be obtained in the least squares sense, thus solving the following optimization problem[1]:

$$\arg\min_{\Pi}\sum_{h=1}^{N}\left|G_{np}\left(jh\omega_n\right)-G_p\left(jh\omega_n,\Pi\right)\right|^2 \qquad (5)$$

The considerations reported in Section II.A suggest employing a transfer function $G_p(s,\Pi)$ having three zeros and a pole. In this case, solving (5) under the minimum phase constraint does not result in a very good fit. This is somewhat expected, since the equivalent circuit depicted in Fig. 2 represents an approximated, lumped-parameter model of the VT which is based on reasonable simplifications. On the other hand, excellent results can be obtained while employing a parametric transfer function having two poles and a zero. Obtained magnitude and phase responses are reported in Fig. 5 and Fig. 6, respectively.

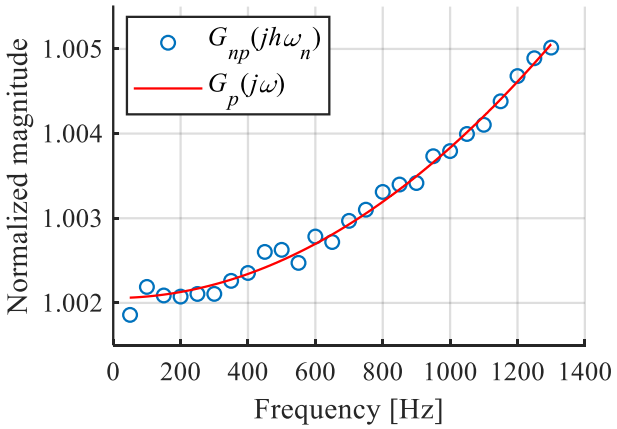

Fig. 5. Normalized magnitude response: nonparametric and parametric inverse FRFs.

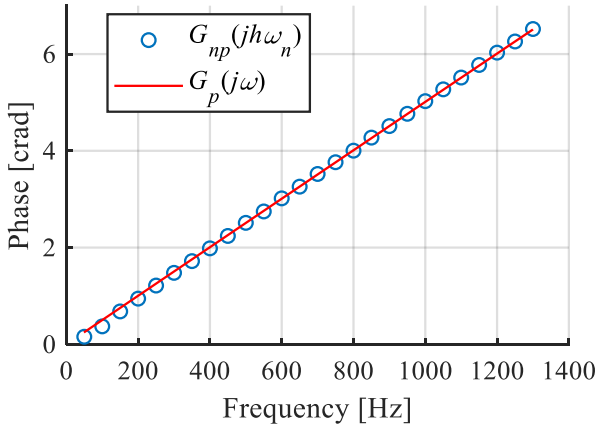

Fig. 6. Phase response: nonparametric and parametric inverse FRFs.

According to the proposed approach, the FRF has to be measured for each VT specimen. One may also consider using the same FRF for all nominally equal VTs in a batch. However, significantly lower performance is expected since the FRF is affected by parasitic effects that are not generally controlled during the production process.

[1] The nonlinear and non-convex optimization problem has been solved using the function tfest of the Matlab System Identification Toolbox.

V. Experimental Results

A. Test conditions: single superimposed harmonic

Having identified the nonparametric and parametric inverse FRFs $G_{np}(jh\omega_n)$ and $G_p(j\omega)$ that allow compensating the filtering behavior of the VT, now the target is assessing the accuracy in measuring harmonic synchrophasors that can be reached thanks to the proposed approach. Firstly, the class of primary voltage signals used to test the harmonic disturbance rejection for class P compliance [24] has been considered. Each signal consists of a fundamental component having rated amplitude and frequency f_0, superimposed to a single hth order harmonic (h ranging from 2 to 25), whose amplitude is equal to 1% of the fundamental. Eight different harmonic phase angles evenly distributed between $-\pi$ and π have been considered. The possible values f_0 for the fundamental frequency have been selected to have an integer number M of samples per period.

The signals have been applied to the VT under test by using the voltage generator, and the resulting steady-state primary and secondary voltage waveforms have been measured for P=100 periods. Through averaging over the acquired periods, the impact of noise can be heavily mitigated: under the usual assumptions, a 20 dB improvement in the SNR is achieved. In this way, it is possible to highlight the impact of the VT, of the compensation technique and of the algorithm employed to extract harmonic synchrophasor, while the effect of noise is virtually negligible with respect to the others. The samples of the acquired secondary voltage waveform $v_2(t)$ have been prefiltered, decimated by a factor 10 and sent to the synchrophasor estimation algorithm. The estimates of the primary voltage synchrophasors $V_{1,E}(h)$ have been obtained by using either the nominal ratio $K_n=V_{1n}/V_{2n}$, the nonparametric or parametric inverse FRF ($G_{np}(jh\omega_n)$ or and $G_p(j\omega)$, respectively).

Very accurate estimates of the harmonic synchrophasor $V_1(h)$ can be obtained by using the output of the voltage divider connected to the primary side and computing the DFT over M samples. This measurement is employed as a reference value. For each injected harmonic, the harmonic Total Vector Error (TVE) for harmonic order h has been evaluated as:

$$\mathrm{TVE}(h)=\frac{\left|V_{1,\mathrm{E}}(h)-V_1(h)\right|}{\left|V_1(h)\right|} \qquad (6)$$

B. Test conditions: realistic voltage waveforms

The previous tests have been carried out by supplying the VT with a set of simple signals that allows easily evaluating the accuracy in harmonic synchrophasor measurement. However, such waveforms are not representative of a generic operating condition of the distribution grid since several harmonics could be present simultaneously.

Standard EN50160 [35] defines the limits for harmonic voltage amplitudes in public distribution grids; values are reported in Table III. The standard states that, considering a one-week observation period, the 10-minute rms value of each harmonic component shall be below the corresponding limit for at least 95% of the time. Furthermore, the 10-minute rms voltage shall be within 90% and 110% of its rated value. These limits can be used to define a new class of realistic voltage waveforms, resembling those typically found in distribution grids. Harmonic amplitudes are considered as random variables having Rayleigh distributions; the 95$^{\text{th}}$

percentile value corresponds to the respective limit. The fundamental magnitude is supposed to be normally distributed having expected amplitude equal to its rated value and standard deviation so that it falls between ±10% of the rated value with 95% probability. The standard [35] does not provide information about phases, which are assumed to be independent and uniformly distributed between $-\pi$ and π.

TABLE III. HARMONIC VOLTAGE AMPLITUDE LIMITS (PERCENTAGES OF THE FUNDAMENTAL COMPONENT)

Odd harmonics				Even harmonics	
k	P_k	k	P_k	k	P_k
3	5.0 %	15	0.5 %	2	2.0 %
5	6.0 %	17	2.5 %	4	1.0 %
7	5.0 %	19	1.5 %	6	0.5 %
9	1.5 %	21	0.5 %	8	0.5 %
11	3.5 %	23	1.5 %	10	0.5 %
13	3.0 %	25	1.5 %	14÷24	0.5 %

A set of 200 primary voltage spectra have been obtained by sampling the previously defined probability density functions. Having selected a value of the fundamental frequency f_0 (an integer number M of samples per fundamental period is assumed as before) the waveforms can be synthesized and applied to the VT under test. P=100 periods of the primary and secondary voltage waveforms under steady state conditions have been collected and averaged. Also in this case, the primary voltage harmonic synchrophasors have been reconstructed by using K_n, $G_{np}(jh\omega_n)$ or $G_p(j\omega)$. The reference values of the primary voltage synchrophasors are extracted through DFT computed over M samples of the primary voltage waveforms.

According to the previously introduced probability density functions of the harmonic amplitudes, their values could be extremely small. Therefore, the value of the harmonic TVE defined as in (6) may become extremely large. For this reason, performance has been evaluated by introducing a new metric:

$$\mathrm{TVE}_{\mathrm{exp}}(h)=\frac{\left|V_{1,\mathrm{E}}(h)-V_1(h)\right|}{V_{1,\mathrm{exp}}(h)} \tag{7}$$

Where $V_{1,\mathrm{exp}}(h)$ represents the expected amplitude of the h-th harmonic, which can be easily computed from the statistical features characterizing the class of excitation signals.

C. Test results

The first tests have been performed by considering rated fundamental frequency and using the same assumptions as in Section V.A. The synchrophasor estimation algorithm runs at f_{sa}=10 kHz and thus a prefiltering and 10-to-1 downsampling stage is adopted at the estimation procedure input. For each harmonic component, the maximum TVE obtained with the different phase angles has been computed, following the same steps as in [23], to compare and assess the estimations. Fig. 7 shows the results in terms of percent TVE when three different approaches for compensation are adopted (N_{c1}=N_{c2}=5). The first two (indicated as K_n and $G_{np}(jh\omega_n)$, respectively) are the same adopted in [23], that is the simple compensation with the nominal VT ratio K_n and the compensation obtained through the non-parametric FRF measured on the nominal harmonic grid. The third one ($G_p(j\omega)$ in the figure) uses the parametric FRF estimated and represents the result of the full integration of the harmonic synchrophasor estimation and of the compensation process.

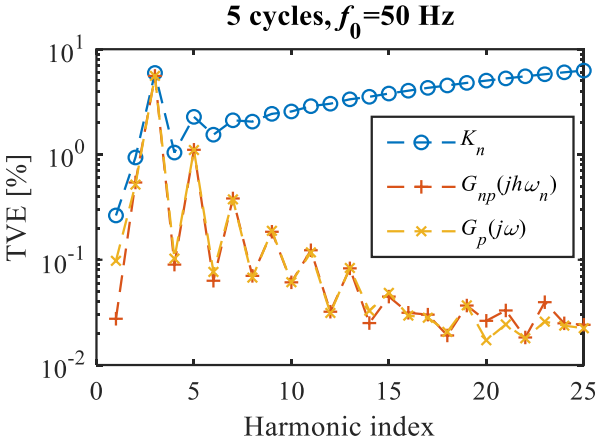

Fig. 7. Maximum TVE for the estimated harmonic syncrophasors, f_0=50 Hz.

Under nominal frequency and steady-state conditions, the synchrophasor estimation algorithm operates in synchronous sampling conditions and returns virtually error-free measurements (for both harmonics and frequency) and thus all the errors can be attributed to the VT. As indicated by the blue line, the uncompensated VT response (only nominal ratio is used to obtain $V_{1,\mathrm{E}}$) leads to an error that increases with the harmonic order and resulting in unacceptable performance. For example, the 25th order harmonic is measured with a TVE reaching 6.3 %. The fundamental component is characterized by 0.26 % TVE, of course compliant with the accuracy class of the considered VT. When compensation is employed, evident advantages emerge and the TVE(h) drops even below 0.05 %. This is particularly effective where the filtering behavior of the VT is stronger.

As expected, at nominal frequency the two compensation approaches behave very similarly. The only significant difference is at nominal frequency, where the estimation of $G_{np}(j\omega_n)$ is extremely accurate, while $G_p(j\omega_n)$ is somewhat less precise because it suffers from undermodeling effects (the FRF model does not allow a perfect fitting of the experimental data). On the other hand, harmonic frequency measurements are slightly affected by the impact of noise in the FRF estimations.

Furthermore, it is worth highlighting that the trend of TVE is not smooth: peaks are present at low-order, odd harmonics. The reason is the odd nonlinearity introduced by the VT (because of the odd-symmetric hysteresis loop), resulting in odd-order harmonic distortion produced by the strong fundamental component.

As highlighted also in [23], the FRF compensation is way less effective when looking at low-order odd harmonics, namely the most affected by nonlinearity. When the 3rd order harmonic synchrophasor is taken into account, maximum TVE is reduced only from 5.95 % to 5.58%; nonlinear effects progressively fade out as harmonic order increases. Therefore, the nonlinearities introduced by the VT represent the performance bottleneck under this operating condition.

Tests have been repeated by considering a deviation with respect to nominal frequency (off-nominal frequency conditions). The same fundamental frequencies used in [23] are employed here for the primary voltage signals. In

particular, 204 samples per cycle at sampling rate f_{sa} are considered, thus corresponding to fundamental frequency $f_0 \cong 49.02$ Hz; Fig. 8 shows the results.

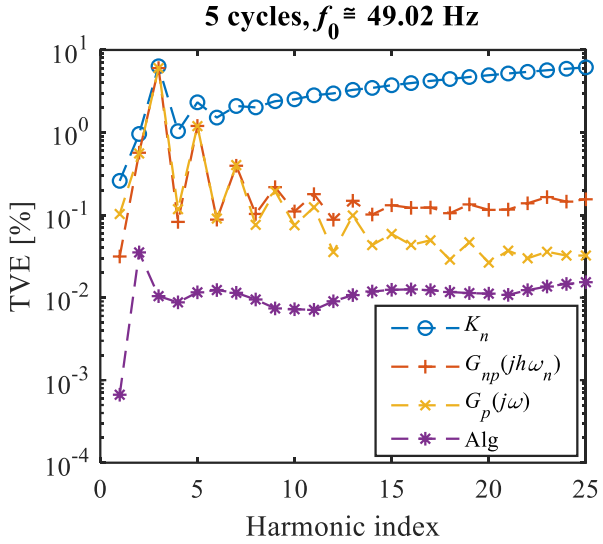

Fig. 8. Maximum TVE for the estimated harmonic syncrophasors, $f_0 \cong 49.02$ Hz.

Since the harmonic synchrophasor estimation algorithm can no longer be considered to have a negligible impact on the measurements, its intrinsic error contribution ('Alg' purple line) is also shown. These maximum TVE values are obtained by directly applying the estimation algorithm to the primary voltage signals (as if the VT were ideal). This gives a bottom TVE line that represents the best possible estimates. The compensation appears essential to achieve good measurement performance, but it is interesting to notice that, in this case, the parametric compensation enables a much more accurate measurement of higher order harmonics. For example, considering harmonic indexes above 10, the error reduction is higher than 30 % and goes up to 79 % for the 25th order harmonic. As mentioned before, the errors for low order, odd harmonics are dominated by nonlinearities and thus the FRF compensation cannot improve accuracy.

With the parametric compensation, the TVE values for all the harmonics are similar to those achieved under rated frequency conditions (Fig. 7), whereas non-parametric approach degrades for higher order harmonics. The VT is the predominant uncertainty source and, thus, refining its compensation means pushing the performance towards the lower bound set by algorithm (below 0.02 %). Similar results can be found, for instance, when a fundamental tone with 196 samples per cycle (thus resulting in $f_0 \cong 51.02$ Hz) is considered.

Another significant test has been performed using the class of waveforms defined in Section V.B. Fig. 9 shows, with the same fundamental frequency as in Fig. 8, the results in terms of rms TVE_{exp} (defined in (7)) calculated over the 200 random signals extracted from EN 50160 limits (for each condition the maximum TVE is considered). The conclusions are similar to the previous case. Once more, the compensation is key to improve performance at higher order harmonics, and the parametric FRF approach allows further error reduction (up to 56 % at the 25th order harmonic).

To stress the overall measurement chain, a white uniform noise (AWUN) at a SNR of 70 dB has also been added to the secondary voltage signals. Fig. 10 reports the TVE results as the maximum rms values across the 8 different phases for the case of single harmonic test and off-nominal fundamental frequency (as in Fig. 8). The results are influenced by the additive noise and thus the ideal algorithm error is not meaningful and thus no longer reported.

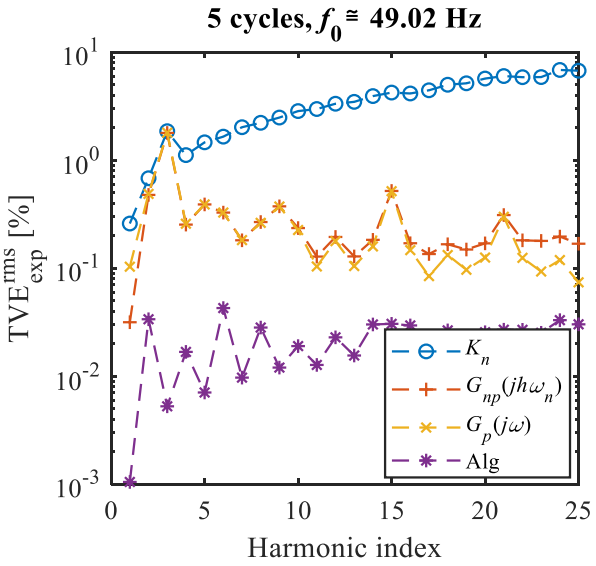

Fig. 9. EN 50160 test case: rms TVE_{exp} for the estimated harmonic syncrophasors, $f_0 \cong 49.02$ Hz.

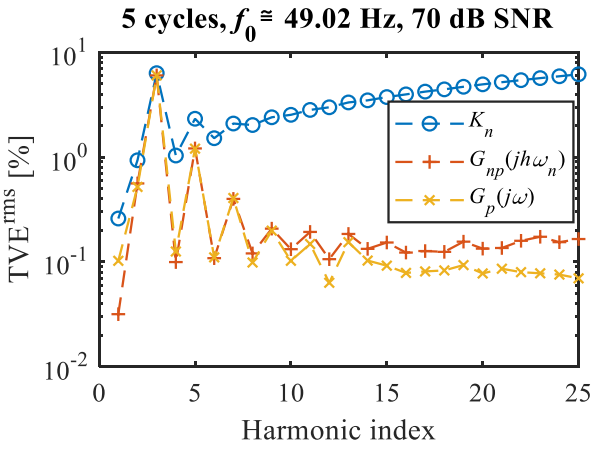

Fig. 10. Rms TVE for the estimated harmonic syncrophasors, $f_0 \cong 49.02$ Hz, AWUN with 70 dB SNR.

The impact of the compensation is clearly visible and the error reduction obtained with the parametric approach is still noticeable albeit it is smaller than before. From harmonic index 10, the error reduction is above 20 % and up to 58 % and it shows the same behavior as in the previous tests. To reduce the influence of the noise, it is possible to leverage the duration of the windows used for the synchrophasors estimation. With $N_{c1}=N_{c2}=10$ nominal cycles, the performance of the parametric compensation is improved: in this case, the parametric approach allows an error reduction up to 69 % with respect to the nonparametric compensation (23rd order harmonic). The price to pay is that algorithm latency becomes about two times higher, due to the longer time window, and the computational burden is almost doubled. In addition, the capability to follow dynamic conditions could be jeopardized. The difference of the TVE values for the non-parametric approach is instead negligible with respect to Fig. 10, thus indicating that in this case

performance is capped by the inaccurate compensation technique. Tests in the presence of noise have been performed also for the EN 50160 waveforms. The rms TVE_{exp} graphs patterns are similar to those obtained without noise. Error reduction using the parametric FRF compensation is up to 41 % for 5-cycle estimation (harmonic order 23) and 52 % for 10 cycles (harmonic order 25).

It is worth noting that the results confirm the outcomes of the analysis carried out in [23], concerning the impact of linear compensation and the influence of nonlinearities on the different harmonic orders. In particular, the nonlinearity introduced by the inductive VT has an impact on the measurement of low-order harmonic synchrophasors (particularly on the 3rd order one). For higher accuracy, the synchrophasor estimation algorithm could be integrated with a proper technique able to mitigate these nonlinear effects. Of course, it may significantly increase computational complexity.

In conclusion, this study points out the importance of the integration between estimation algorithm, VT and compensation technique while addressing the different uncertainty sources. It is possible to design the estimation algorithm depending on the available compensation data and it is also clear that, under some circumstances and for specific harmonics, it is not beneficial to overdesign the algorithm if the uncertainty contribution due to the VT is not properly addressed. On the other side, a VT compensation that does not consider the estimated frequency does not permit to take full advantage of the potentialities of the measurement process.

VI. Conclusion

This paper has proposed the idea of an integrated design of harmonic synchronized measurement algorithm with VT compensation to address the two main sources of measurement errors: VT and signal model. Both the VT and the employed algorithm may significantly contribute to the TVE for different harmonic orders and test conditions. The results show that VT compensation can be seen not only as a static post-processing to add to the instrument output, but as measurement stage that leverages the outputs of the harmonic synchrophasor estimation algorithm. Hence, in order to achieve best overall performance in the most effective way, the algorithm, the VT and the mapping function between secondary and primary side quantities have to be jointly and carefully selected and defined to meet the required accuracy constraints. The method has been experimentally validated on an inductive VT but, thanks to the black-box approach, it can be applied to other types of voltage transducer.

References

[1] J. Arrillaga and N. R. Watson, Power System Harmonics. Hoboken, NJ, USA: Wiley, 2003.

[2] A. Meliopoulos, F. Zhang, and S. Zelingher, “Power system harmonic state estimation,” *IEEE Trans. Power Del.*, vol. 9, no. 3, pp. 1701–1709, Jul. 1994.

[3] C. Rakpenthai, S. Uatrongjit, N. R. Watson and S. Premrudeepreechacharn, "On Harmonic State Estimation of Power System With Uncertain Network Parameters," *IEEE Trans. Power Syst.*, vol. 28, no. 4, pp. 4829-4838, Nov. 2013.

[4] C. F. M. Almeida and N. Kagan, "Harmonic state estimation through optimal monitoring systems," *IEEE Trans. Smart Grid*, vol. 4, no. 1, pp. 467-478, March 2013.

[5] L. Cristaldi and A. Ferrero, "A digital method for the identification of the source of distortion in electric power systems," *IEEE Trans. Instrum. Meas*., vol. 44, no. 1, pp. 14-18, Feb. 1995.

[6] A. Cataliotti and V. Cosentino, "A New Measurement Method for the Detection of Harmonic Sources in Power Systems Based on the Approach of the IEEE Std. 1459–2000," *IEEE Trans. Power Del.*, vol. 25, no. 1, pp. 332-340, Jan. 2010.

[7] D. Carta, C. Muscas, P. A. Pegoraro and S. Sulis, "Identification and Estimation of Harmonic Sources Based on Compressive Sensing," *IEEE Trans. Instrum. Meas.*, vol. 68, no. 1, pp. 95-104, Jan. 2019.

[8] A. G. Phadke and J. S. Thorp, *Synchronized Phasor Measurements and Their Applications*. New York: Springer, 2008.

[9] A. Carta, N. Locci, and C. Muscas. GPS-based system for the measurement of synchronized harmonic phasors. *IEEE Trans. Instrum. Meas.*, vol 58, no. 3, pp. 586–593, 2009.

[10] *Instrument transformers – the use of instrument transformers for power quality measurement*, document IEC TR 61869-103, 2012.

[11] *Instrument transformers - Part 3: Additional requirements for inductive voltage transformers*, document IEC 61869-3:2011, 2011.

[12] M. Kaczmarek, "Measurement error of non-sinusoidal electrical power and energy caused by instrument transformers," in *IET Generation, Transmission & Distribution*, vol. 10, no. 14, pp. 3492-3498, Nov. 2016.

[13] M. I. Samesima, J. C. de Oliveira and E. M. Dias, "Frequency response analysis and modeling of measurement transformers under distorted current and voltage supply," *IEEE Trans. Power Del.*, vol. 6, no. 4, pp. 1762-1768, Oct 1991.

[14] M. Klatt, J. Meyer, M. Elst and P. Schegner, "Frequency Responses of MV voltage transformers in the range of 50 Hz to 10 kHz," in *Proc. Int. Conf. on Harmonics and Quality of Power*, 2010, pp. 1-6.

[15] M. Faifer, C. Laurano, R. Ottoboni, S. Toscani, M. Zanoni, “Characterization of Voltage Instrument Transformers Under Non-Sinusoidal Conditions Based on the Best Linear Approximation”, *IEEE Trans. Instrum. Meas*., vol. 67, no. 10, pp. 2392-2400, Oct. 2018.

[16] G. Crotti, D. Gallo, D. Giordano, C. Landi, M. Luiso and M. Modarres, "Frequency Response of MV Voltage Transformer Under Actual Waveforms," *IEEE Trans. Instrum. Meas.*, vol. 66, pp. 1146-1154, June 2017.

[17] M. Faifer, C. Laurano, R. Ottoboni, S. Toscani, M. Zanoni, G. Crotti, D. Giordano, L. Barbieri, M. Gondola and P. Mazza, "Overcoming Frequency Response Measurements of Voltage Transformers: An Approach Based on Quasi-Sinusoidal Volterra Models," *IEEE Trans. Instrum. Meas*., vol. 68, no. 8, pp. 2800-2807, Aug. 2019.

[18] C. Buchhagen, L. Hofmann and H. Däumling, "Compensation of the first natural frequency of inductive medium voltage transformers," in *Proc. IEEE Int. Conf. on Power System Technology*, 2012, pp. 1-6.

[19] L. Kadar, P. Hacksel and J. Wikston, "The effect of current and voltage transformers accuracy on harmonic measurements in electric arc furnaces," *IEEE Trans. on Ind. Appl.*, vol. 33, no. 3, pp. 780-783, May/Jun 1997.

[20] B. Boulet, L. Kadar and J. Wikston, "Real-time compensation of instrument transformer dynamics using frequency-domain interpolation techniques," in *Proc. IEEE Instrumentation and Measurement Technology Conf.*, 1997, pp. 285-290.

[21] A. Cataliotti, V. Cosentino, G. Crotti, A. Delle Femine, D. Di Cara, D. Gallo, D. Giordano, C. Landi, M. Luiso, M. Modarres, G. Tinè, "Compensation of Nonlinearity of Voltage and Current Instrument Transformers," *IEEE Trans. Instrum. Meas.*, vol. 68, no. 5, pp. 1322-1332, May 2019.

[22] S. Toscani, M. Faifer, A. M. Ferrero, C. Laurano, R. Ottoboni and M. Zanoni, "Compensating Nonlinearities in Voltage Transformers for Enhanced Harmonic Measurements: the Simplified Volterra Approach," *IEEE Trans. Power Del.*, to be published.

[23] C. Laurano, S. Toscani, M. Zanoni, P. Castello, C. Muscas and P. A. Pegoraro, "Combined Impact of Voltage Transformer and Estimation Algorithm on Harmonic Synchrophasors Measurements," in *Proc. IEEE Int. Instrumentation and Measurement Technology Conf.*, Dubrovnik, Croatia, 2020, pp. 1-6.

[24] Angioni *et al.*, *Phasor Measurement Units and Wide Area Monitoring Systems*, 1st ed., A. Monti, C. Muscas and F. Ponci, Eds. Academic Press, 2016.

[25] L. Chen, W. Zhao, F. Wang, and S. Huang, “Harmonic phasor estimator for P class phasor measurement units,” *IEEE Trans. Instrum. Meas*., May 2019.

[26] IEC – International Electrotechnical Commission, IEC 61000-4-30, “Electromagnetic Compatibility – Part 4-30: Testing and Measurement Techniques – Power Quality Measurement methods”, Edition 2.0, 2008.

[27] IEEE/IEC International Standard - Measuring relays and protection equipment - Part 118-1: Synchrophasor for power systems - Measurements," in *IEC/IEEE 60255-118-1:2018*, pp.1-78, 19 Dec. 2018.

[28] M. Chakir, I. Kamwa, and H. Le Huy, ‘‘Extended C37.118.1 PMU algorithms for joint tracking of fundamental and harmonic phasors in stressed power systems and microgrids,’’ *IEEE Trans. Power Del*., vol. 29, no. 3, pp. 1465–1480, Jun. 2004.

[29] G. Frigo, A. Derviškadić, P. A. Pegoraro, C. Muscas and M. Paolone, "Harmonic Phasor Measurements in Real-World PMU-Based Acquisitions," 2019 *IEEE International Instrumentation and Measurement Technology Conf.*, Auckland, New Zealand, 2019, pp. 1-6.

[30] M. A. Platas-Garza and J. A. de la O Serna, "Dynamic Harmonic Analysis Through Taylor–Fourier Transform," in *IEEE Transactions on Instrumentation and Measurement*, vol. 60, no. 3, pp. 804-813, March 2011.

[31] S. K. Jain, P. Jain, and S. N. Singh, “A fast harmonic phasor measurement method for smart grid applications*,” IEEE Trans. Smart Grid*, vol. 8, no. 1, pp. 493–502, Jan. 2017.

[32] R. Ferrero, P. A. Pegoraro and S. Toscani, "Dynamic fundamental and harmonic synchrophasor estimation by Extended Kalman filter," *2016 IEEE Int. Workshop on Applied Measurements for Power Systems*, Aachen, 2016, pp. 1-6.

[33] M. Faifer, R. Ottoboni, S. Toscani, C. Cherbaucich and P. Mazza, "Metrological Characterization of a Signal Generator for the Testing of Medium-Voltage Measurement Transducers," *IEEE Trans. Instrum. Meas.*, vol. 64, no. 7, pp. 1837-1846, July 2015.

[34] R. Pintelon, J. Schoukens, “System Identification. A frequency domain approach,” 2nd ed., Boston, MA, USA, Wiley, 2012.

[35] *Voltage characteristics of electricity supplied by public distribution networks*, Standard EN 50160, 2010.